

**EFFECT OF CaO, CuO AND V₂O₅ ON BARIUM ZINC TANTALATE (BZT)
DIELECTRIC PROPERTIES**

by

HIDAYANI BT JAAFAR

**Thesis submitted in fulfillment of the
requirements for the degree of
Master of Science**

JULY 2011

ACKNOWLEDGEMENT

In the name of Allah, the Most Gracious, Most Merciful.

I would like to express my sincere gratitude to the Professor Ahmad Fauzi Mohd Noor, the Dean of School of Materials and Mineral Resources Engineering, Universiti Sains Malaysia for providing me a platform to gain a lot of valuable knowledge that I can apply in the future. I also would like to express my grateful to USM for providing me the USM Fellowship for the past one year and four months.

I am deeply indebted to my dedicated main supervisor, Professor Hj. Zainal Arifin Hj. Ahmad and my co-supervisor Associate Professor Mohd Fadzil Ain for their guidance, advice, stimulating suggestions and comments in all the time of research and writing of this thesis. Thank you so much for unending help through the course of my research.

Special thanks to my parents, En. Jaafar bin Md. Yusof and Pn. Asmah bt Hedzir and also to my sisters. Thank you for your support and encouragements. I also would like to thank to all technicians for their guidance and assistance especially En. Sharul Ami b. Zainal Abidin, En. Abdul Rashid b. Selamat, En. Mohd. Shahid b. Abd. Jalal and En. Mokhtar b. Mohamad. Their help will always be remembered. I would like to express my thanks to my beloved friends and colleagues who supported me in my research.

TABLES OF CONTENTS

ACKNOWLEDGMENTS	ii
TABLE OF CONTENTS	iii
LIST OF TABLES	viii
LIST OF FIGURES	ix
LIST OF ABBREVIATIONS	xiv
LIST OF SYMBOLS	xv
ABSTRAK	xvi
ABSTRACT	xvii
CHAPTER 1 - INTRODUCTION	
1.1 Introduction	1
1.2 Problem Statement	6
1.3 Research Objective	8
1.4 Scope of Work	9
CHAPTER 2 – LITERATURE REVIEW	
2.1 Microwave Communications	11
2.1.1 Dielectric Resonators (DR)	12
2.1.2 Dielectric Resonator Antenna (DRA)	13
2.1.2.1 Effect of DRA Height and Shape	14
2.1.2.2 The Hemispherical DRA	16

2.1.2.3 The Rectangular DRA	17
2.1.2.4 The Cylindrical DRA	18
2.1.3 Dielectric Microwave Properties	19
2.1.3.1 Dielectric Resonance Frequency (f)	19
2.1.3.2 Dielectric Constant (ϵ_r)	20
2.1.3.3 Dielectric Loss ($\tan \delta$)	22
2.1.3.4 Minimum Return Loss	23
2.1.3.5 Bandwidth (BW)	24
2.2 Perovskite Structure	25
2.2.1 High Q Perovskite Ceramics	27
2.2.2 BZT	30
2.3 Influence of Dopants in BZT	30
2.3.1 Influence of CaO, CuO and V ₂ O ₅ on Microwave Dielectric Properties	34
2.4 Synthesis of BZT	36
2.4.1 Solid State Method	37
2.4.2 Sol gel	39
2.4.3 Hydrothermal	41
2.4.4 Chemical Coprecipitation	41
2.4.5 Citrate Precursor Gel	42
2.4.6 Selection of Synthesis Method	42
2.5 Mixing	43
2.6 Calcination	46

2.7 Shaping	47
2.8 Sintering	47
CHAPTER 3 - METHODOLOGY	
3.1 Analysis of Raw Materials	51
3.2 Experimental Design	52
3.2.1 General Flowchart of Experiment	53
3.3 Investigation of the Lowest Calcination Temperature to Produce Single Phase of BZT using Solid State Method (Phase 1)	54
3.3.1 Preparation of BZT Powder	54
3.3.2 Mixing	54
3.3.3 Calcination Process	55
3.4 Reducing the Sintering Temperature of BZT by Doping with CaO, CuO and V ₂ O ₅ (Phase 2)	56
3.4.1 BZT without Dopant Process	56
3.4.1.1 Uniaxial pressing	56
3.4.1.2 Sintering Process	57
3.4.2 BZT with Dopant Process	58
3.5 Studying of the Microwave Dielectric Properties of BZT Doped with CaO, CuO and V ₂ O ₅ , respectively (Phase 3)	60

3.6 Characterization for BZT and Doped BZT	60
3.6.1 Differential Thermal Analysis-Thermal Gravimetry Analysis (DTA-TGA)	60
3.6.2 XRD	61
3.6.3 Shrinkage Test	62
3.6.4 Measurement of Bulk Density and Porosity by using Archimedes Principle	62
3.6.5 Microstructure Analysis	63
3.6.6 Microwave Dielectric Properties Measurement	64
3.6.6.1 Dielectric properties formulation	65

CHAPTER 4 - RESULTS AND DISCUSSION

4.1 Introduction	67
4.2 Raw Materials Characterization	67
4.2.1 BaCO ₃ Powder	67
4.2.2 ZnO Powder	69
4.2.3 Ta ₂ O ₅ Powder	70
4.2.4 CaO Powder	71
4.2.5 CuO Powder	72
4.2.6 V ₂ O ₅ Powder	73
4.3 Investigation of the Lowest Calcination Temperature to Produce Single Phase of BZT using Solid State Method (Phase 1)	74

4.3.1 Determination of Calcination Temperature Range via DTA-TGA analysis	74
4.3.2 XRD	76
4.3.3 Density	81
4.3.4 Particle Size and Morphology	82
4.3.5 Energy Dispersive Spectroscopy (EDS) Analysis and Determination of BZT Ratio	83
4.3.6 Conclusion for the Lowest Calcination Temperature to Produce Single Phase of BZT	86
4.4 Reducing the Sintering Temperature of BZT by Doping with CaO, CuO and V ₂ O ₅ (Phase 2)	86
4.4.1 Analysis Result for Sintering Temperature of Pure BZT	86
4.4.1.1 XRD	86
4.4.1.2 Surface Morphology	88
4.4.1.3 Density and Porosity	90
4.4.1.4 Conclusion for the Sintering Temperature of Pure BZT	91
4.4.2 Determination of the Lowest Sintering Temperature for Doped BZT	91
4.4.3 Comparison of the Characteristic Between Pure BZT at 1350°C and Optimum Sintering Temperature of Doped BZT at 1250°C	92

4.4.3.1 Shrinkage Analysis	96
4.3.3.2 Density Analysis	97
4.3.3.3 Structure Analysis	99
4.3.3.4 Surface morphology	106
4.4 Studying of the Microwave Dielectric Properties of BZT Doped with CaO, CuO and V ₂ O ₅ , respectively (Phase 3)	111
4.4.1 Measurement for Microwave Dielectric Properties	111
4.4.2 Resonance Frequency (<i>f</i>)	112
4.4.3 Dielectric Constant (ϵ_r)	114
4.4.4 Dielectric Loss ($\tan \delta$)	117
4.4.5 Percent of Bandwidth (% BW)	118
4.4.6 Minimum Return Loss	119
CHAPTER 5 – CONCLUSION AND RECOMMANDATION	
5.1 Conclusion	121
5.2 Recommendation	122
REFERENCES	123
APPENDIX A	129
APPENDIX B	133

LIST OF TABLES

Table 2.1:	Types of dielectric materials in microwave communications	27
Table 2.2:	Microwave dielectric properties of BZT with dopants	33
Table 2.3:	Research on BZT synthesis by various methods	37
Table 3.1:	Raw materials that have been used in doped BZT synthesis	51
Table 4.1:	Value of lattice parameter, c^*/a^* ratio, percent of BZT perovskite, density and particle size with different calcinations temperature	79
Table 4.2:	EDS analysis and ratio determination for BZT powders	84
Table 4.3:	List of difference density along with visual observation for sintering temperature at 1200°C, 1250°C, and 1300°C	93
Table 4.4:	The comparison of density between pure BZT (1350°C) and doped BZT (1250°C)	98
Table 4.5:	f of (BZT+CaO), (BZT+CuO) and (BZT+V ₂ O ₅)	113

LIST OF FIGURES

Figure 2.1	Microwave spectrum and applications	12
Figure 2.2:	Return loss for antenna with two samples different height	15
Figure 2.3:	Return loss for antenna with two samples different BW	15
Figure 2.4:	Hemispherical DRA	16
Figure 2.5:	Rectangular DRA	17
Figure 2.6:	Cylindrical DRA	18
Figure 2.7:	The wavelength is reduced by factor of $\sqrt{\epsilon_r}$ when the waves enter the dielectric material	20
Figure 2.8:	Frequency dependence of polarization process and peak power losses	21
Figure 2.9:	Thickness effect for the DR towards return loss. (a) 2 mm, (b) 2.5 mm, and (c) 3 mm	23
Figure 2.10:	Measurement of BW based from the resonance frequency	25
Figure 2.11:	Ordered perovskite of stoichiometry $A(B_{1/3}B'_{2/3})O_3$ with B and B' planes alternating in a 1:1 ratio along the perovskite subcell (111) direction	26
Figure 2.12:	Crystal structure BZT (a) Disorder, and (b) Order	29
Figure 2.13:	Particle arrangement in two dimension mixture	44

Figure 2.14:	Ceramics microstructure during sintering; (a) Loose of particle size, (b) Early stage, (c) Intermediate stage, and (d) Final stage	49
Figure 3.1:	Flowchart of the preparation for pure BZT and doped BZT	53
Figure 3.2:	Calcination profile for powder mixing	56
Figure 3.3:	Sintering profile for pure BZT samples	57
Figure 3.4:	Figure 3.4: (a) Temperature 1200°C/ 4 hours soaking time, with dusty surface and crack on pellet surface, (b) 1250°C/ 4 hours soaking time with fully sintered without any crack and, (c) 1300°C/ 4 hours soaking time with shattered pellet after sintering	59
Figure 3.5:	Heating profile for TGA/DTA	61
Figure 3.6:	DRA mounted on microstrip	64
Figure 3.7:	Example of f for DR	65
Figure 4.1:	XRD diffraction pattern of BaCO ₃ powder was identified as a single phase of BaCO ₃ (ICDD no. 98-006-2998)	68
Figure 4.2:	Particle size analysis for BaCO ₃	68
Figure 4.3:	XRD diffraction pattern of ZnO powder was identified as a single phase of ZnO (ICDD no. 98-010-6787)	69
Figure 4.4:	Particle size analysis for ZnO	69
Figure 4.5:	XRD diffraction pattern of Ta ₂ O ₅ powder was identified as a single phase of Ta ₂ O ₅ (ICDD no. 98-006-8019)	70
Figure 4.6:	Particle size analysis for Ta ₂ O ₅	70

Figure 4.7:	XRD diffraction pattern of CaO powder was identified as a single phase of CaO (ICDD no. 98-005-7282)	71
Figure 4.8:	Particle size analysis for CaO	71
Figure 4.9:	XRD diffraction pattern of CuO powder was identified as a single phase of CuO (ICDD no. 98-005-9310)	72
Figure 4.10:	Particle size analysis for CuO	72
Figure 4.11:	XRD diffraction pattern of V ₂ O ₅ powder was identified as a single phase of V ₂ O ₅ (ICDD no. 98-006-6957)	73
Figure 4.12:	Particle size analysis for V ₂ O ₅	73
Figure 4.13:	TG and DTA curves for the mixture BaCO ₃ -ZnO-Ta ₂ O ₅	75
Figure 4.14:	XRD patterns of BZT were prepared by solid state reaction. Insert shows peaks at 23° to 27° of 2θ°	77
Figure 4.15:	Lattice parameters as a function of calcination temperatures	78
Figure 4.16:	<i>c*/a*</i> ratio as a function of calcination temperatures	80
Figure 4.17:	Percent of perovskite phase content in BZT powders	80
Figure 4.18:	Density versus calcination temperatures	81
Figure 4.19:	Particle size of BZT powders versus calcination temperatures	82
Figure 4.20:	Morphology of BZT powders calcined at (a) 750°C, (b) 1050°C, (c) 1150°C, and (d) 1250°C	85
Figure 4.21:	XRD analysis for BZT sintered at temperature 1250, 1300 and 1350°C. Insert shows peaks at 27° to 36° for Ba _{5.5} Ta _{21.8} O ₆₀ , and BZT	87

Figure 4.22:	c^*/a^* ratio for BZT sintered at temperature 1250, 1300 and 1350°C and soaking time 4 hours	88
Figure 4.23:	Surface morphology for BZT sintered at temperature 1250, 1300 and 1350°C at 4 hour soaking time	89
Figure 4.24:	Density and porosity for BZT sintered at temperature 1250, 1300, and 1350°C at 4 hours soaking time	90
Figure 4.25:	Diameter shrinkage graph for (BZT + x CaO), (BZT + x CuO), and (BZT + x V ₂ O ₅)	97
Figure 4.26:	XRD pattern for BZT with CaO dopant of 0, 0.1, 0.25, 0.5, 1.0, 1.5, and 2.5 mol%. Insert shows peaks at 24° to 35° of 2 θ ° for BZT and BCZT	101
Figure 4.27:	XRD for BZT with CuO dopant of 0, 0.1, 0.25, 0.5, 1.0, 1.5, and 2.5 mol%. Insert shows peaks at 27° to 42° of 2 θ ° for BZT and CuO	102
Figure 4.28:	XRD pattern for BZT with V ₂ O ₅ dopant of 0, 0.1, 0.25, 0.5, 1.0, 1.5, and 2.5 mol%. Insert shows peaks at 24° to 42° of 2 θ ° for BZT, and V ₂ O ₅	104
Figure 4.29:	Lattice constant for (BZT + x CaO), (BZT + x CuO) and (BZT + x V ₂ O ₅)	105
Figure 4.30:	SEM micrograph of (i) BZT + x CuO (ii) BZT + x CaO, and (iii) BZT + x V ₂ O ₅ for different mol%. a $x = 0$, b $x = 0.1$, c $x = 0.5$, d $x = 1.0$, e $x = 1.5$, f $x = 2.5$	108
Figure 4.31:	Frequency (GHz) versus minimum return loss (dB) graph	112

Figure 4.32:	Effect of dopants on f and ϵ_r versus mol%	114
Figure 4.33:	Effect of grain size towards ϵ_r for doped BZT versus mol%	116
Figure 4.34:	$\tan \delta$ of (BZT + $x\text{CaO}$), (BZT + $x\text{CuO}$) and (BZT + $x\text{V}_2\text{O}_5$) versus x (mol%)	118
Figure 4.35:	%BW of (BZT + $x\text{CaO}$), (BZT + $x\text{CuO}$) and (BZT + $x\text{V}_2\text{O}_5$) versus x (mol%)	119
Figure 4.36:	Minimum return loss of (BZT + $x\text{CaO}$), (BZT + $x\text{CuO}$), and (BZT + $x\text{V}_2\text{O}_5$) versus x (mol%)	120

LIST OF ABBREVIATIONS

DR	Dielectric Resonators
GPS	Global Positioning Systems
BZT	$\text{Ba}(\text{Zn}_{1/3}\text{Ta}_{2/3})\text{O}_3$
BZN	$\text{Ba}(\text{Zn}_{1/3}\text{Nb}_{2/3})\text{O}_3$
BMT	$\text{Ba}(\text{Mg}_{1/3}\text{Ta}_{2/3})\text{O}_3$
FESEM	Field Emission Scanning Electron Microscopy
XRD	X-ray diffraction
RF	Radio frequency
UHF	Ultra high frequency
SHF	Super high frequency
EHF	Extremely high frequency
DRA	Dielectric resonator antenna
WLAN	Wireless local area network
Hz	Hertz
GHz	Giga hertz
MPa	Mega pascal
BW	Bandwidth
HELOS	Helium neon optical system
MPa	Mega pascal
DTA-TGA	Differential Thermal Analysis-Thermal Gravimetry Analysis

LIST OF SYMBOLS

ϵ_r	Dielectric constant
Q	Quality factor
c/a ratio	Lattice distortion
f	Resonance frequency
a	Radius
h	Height
ϕ	Azimuth
r	Radial
z	Axial
d	Thickness
w	Width
Ω	Ohms
R	Resistance
A	Cross sectional area
ρ	Volume resistance
I	Current
λ_d	Wavelength in dielectric
λ	Wavelength in air
t	Tolerance factor
V	Voltage

KESAN CaO, CuO DAN V₂O₅ TERHADAP SIFAT-SIFAT DIELEKTRIK BARIUM ZINK TANTALAT (BZT)

ABSTRAK

BZT mempunyai pemalar dielektrik (ϵ_r) yang tinggi dan lesapan dielektrik ($\tan \delta$) yang rendah. Walau bagaimanapun, suhu pensinteraan yang tinggi diperlukan untuk menghasilkan BZT yang mempunyai sifat-sifat dielektrik yang cemerlang. Oleh itu, bagi mengatasi masalah tersebut, pendopan dilakukan ke atas BZT dan mengkaji kesan pengurangan suhu pensinteran berdasarkan pendopan CaO CuO dan V₂O₅ ke atas BZT. CaO dipilih kerana penggantian Ca menghasilkan struktur baru dan mengelakkan pengurangan sifat-sifat dielektrik pada julat frekuensi yang tinggi. Manakala, penambahan CuO dapat mengelakkan peruapan Zn yang menyebabkan pengurangan sifat-sifat dielektrik. Pemilihan V₂O₅ sebagai bahan dop kerana mempunyai suhu leburan yang rendah. Dalam kajian ini, rekabentuk eksperimen dibahagi kepada tiga bahagian. Bahagian pertama, eksperimen dijalankan bagi menghasilkan fasa tunggal BZT pada suhu yang terendah dan 1150°C menghasilkan keputusan yang terbaik. Fasa kedua, BZT yang terhasil daripada fasa pertama dibahagikan kepada dua, bahan asal BZT yang disinter pada suhu 1350°C dan BZT yang didop, (0.1 hingga 2.5 mol%) dan disinter pada 1250°C. Sampel yang disediakan dianalisis menggunakan analisis XRD, FESEM, ketumpatan dan pengecutan. Fasa ketiga, sifat-sifat dielektrik terhadap kesan pendopan daripada fasa kedua dikaji. BZT + xCaO bertindakbalas menghasilkan BCZT dan menukarkan struktur heksagonal ke kubik. Manakala, BZT yang didop dengan CuO dan V₂O₅ tidak memberi kesan kepada struktur asal. Penambahan mol% bahan daripada 0.1 sehingga 0.5 mol% menghasilkan struktur yang lebih padat. Setiap sampel menunjukkan hasil yang berbeza bergantung kepada mol% bahan didop dimana frekuensi salunan adalah dari 10.3 hingga 14.8 GHz dan kebertelusan dalam julat 26.29 hingga 75.9 serta kehilangan tangen dalam lingkungan 0.04 hingga 0.159.

EFFECT OF CaO, CuO AND V₂O₅ ON BARIUM ZINC TANTALATE (BZT) DIELECTRIC PROPERTIES

ABSTRACT

BZT has high dielectric constant (ϵ_r) and low dielectric loss ($\tan \delta$). However, the formation of BZT using solid state method required high sintering temperature to produce excellent dielectric properties. Therefore, to overcome these problems, other elements were added in BZT and investigate the effect of reducing sintering temperature of BZT by doping with by CaO, CuO and V₂O₅ respectively. CaO was selected as a doping compound because the Ca substitution form a new structured and avoid deteriorated dielectric properties in high frequency range. Meanwhile, adding CuO can avoid Zn evaporation problem which lower the dielectric properties. The selection of V₂O₅ as a doping compound is to improve BZT dielectric since V₂O₅ has a relatively low melting point. In this study, the experimental design is divided into three phases. In the first phase, the experiment was designed to produce the lowest calcination temperature that form single phase of BZT and 1150°C give the best result. For the second phase, BZT produced from the first phase was divided into; pure BZT sintered at 1350°C and doped BZT, (0.1 to 2.5 mol%) sintered at 1250°C. The samples produced were characterized using XRD, FESEM density and shrinkage analysis. In the third phase, the effects of dopants from second phase were investigated on dielectric properties of doped BZT. BZT + xCaO appeared to react to form BCZT and turn from hexagonal to cubic structure. While for BZT doped with CuO and V₂O₅, the structure remains unchanged. Increasing the mol% of dopants from 0.1 to 0.5 mol% produced more compacted structure. Each samples showed a resonance frequency from 10.3 to 14.8 GHz and dielectric constants in the range of 26.29-75.9 and the dielectric loss is 0.04-0.159 depending on the mol% of dopant.

CHAPTER 1

INTRODUCTION

1.1 Introduction

Microwave dielectric materials play an important part in the developing of the satellite communication including Global Positioning Systems (GPS) to environmental monitoring via satellites (Sebastian et al., 2008). The widely research that is related to microwave telecommunication, satellite broadcasting has resulted in an increasing demand for dielectric resonators (DR), which are low loss ceramics pucks used mainly in wireless communication devices (Sebastian et al., 2008). The development of high dielectric constant (ϵ_r), low dielectrics loss ($\tan \delta$) has enabled the production of miniaturized resonators and filters through the use of DR. A DR is an electromagnetic component that exhibits resonance with useful properties for a narrow range of frequencies (Pern et al., 1999). The properties that required for DR are suitable range of resonance frequency (f), low $\tan \delta$, and high ϵ_r . Low $\tan \delta$ or high quality factor (Q) gives a smaller bandwidth (BW) at the f , a lower degree of noise, and less power loss (Muller et al., 2000). Thus, it is important to develop and study dielectrics with a high Q factor in the microwave regime.

Complex oxides are playing important role in the wireless communications and also in particular cellular phone. In the form of the ceramic DR they have had a great impact on the microwave-based wireless communications industry by reducing the size and cost of filter and oscillator components in products ranging from cellular telephones to GPS. Understanding more to the current materials in the aspects of their processing,

synthesis and structure property relationship is needed for further system miniaturization of new ceramics with higher ϵ_r and good temperature stability along with lower $\tan \delta$.

Before the development of complex perovskite dielectric resonators (DR), Cohen et al. (1965) used TiO_2 as a DR. Although it has a high ϵ_r and low $\tan \delta$, it has poor stability of f that prevented its commercial exploitation. The earliest commercialization of DR was started in the early 1970s when the first temperature stable, low $\tan \delta$ barium tetratitanate (BaTi_4O_9) ceramics were developed by Masse et al. (1971). Since then extensive theoretical and experimental work and development of DR materials has occurred.

$\text{Ba}(\text{Zn}_{1/3}\text{Ta}_{2/3})\text{O}_3$ (BZT) is a ceramic composition that contains Ba, Zn, Ta and O elements. Dielectric properties of complex perovskite compounds such as BZT and $\text{Ba}(\text{Zn}_{1/3}\text{Nb}_{2/3})\text{O}_3$ (BZN) have been extensively investigated for their use as DR for satellite communication systems at microwave frequencies >10 GHz (In et al., 1993). BZT is a well-known ceramic material having a high ϵ_r ($\epsilon_r \sim 29$) and high Q ($Q \times f \sim 80,000 - 150,000$ GHz). BZT has a complex perovskite structure and belongs to the family of materials $A(\text{B}'_{1/3}\text{B}''_{2/3})\text{O}_3$ [$A = \text{Ba}$, $\text{B}'_{1/3} = \text{Zn}$, $\text{B}''_{2/3} = \text{Ta}$] used in microwave communication systems (Ioachim et al., 2007).

High sintering temperature above 1500°C or prolonged heat treatment will lead to volatilization of ZnO and the escape of ZnO will lead to poor densification near the surface of the samples (Reaney et al., 2003). The depletion of ZnO also will contribute to the second phase like $\text{Ba}_3\text{Ta}_2\text{O}_8$ and BaTa_2O_6 . The secondary phases that occur in BZT also the factor that causes the Q values factor decrements. The Zn loss during the processing also will decrease the dielectric properties and also play an important role in controlling the crystal structure. Kawashima et al. (1983) suggested

that the increase in Q values might be due to lattice distortion (c^*/a^* ratio) rather than ordering of Zn and Ta cations, porosity or grain size. Zn and Ta cations are ordered, BZT has a hexagonal crystal structure and the c^*/a^* ratio deviates from the value for an ideal hexagonal unit cell ($3^{1/2}/2^{1/2} = 1.2247$) which is called the c^*/a^* ratio. Meanwhile, Koga et al. (2006) said that the Q values of BZT system was found to depend not only on the ordering but also on their ceramic microstructure.

When Zn and Ta cations are disordered over the B-site, the crystal structure of BZT is cubic perovskite with Pm3m space group symmetry. When B-site cations order along the [111] direction of this simple perovskite compound, a hexagonal superlattice is formed with space group $\overline{P3m1}$. This ordering has been investigated for its effect on the microwave Q values. A strong relationship between ordering parameters and microwave Q values in BZT system was experimentally observed by Kawashima et al. (1983) under various heat conditions. They also reported that improvement of the microwave Q values in the BZT system by prolonged sintering and indicated that this Q values improvement corresponded with an increase in cation order of the structure.

Kawashima et al. (1993) reported that to achieve a perfect hexagonal structure at 1350°C takes at least 120 hours. However, Desu and O'Bryan (1985) pointed out that there is another factor at work during these long sintering times, the weight loss occur due to the loss of volatile ZnO. They noted that the c^*/a^* ratio and ordering do not occur simultaneously in the data of Kawashima et al. (1993) as would be expected if the only factor was ordering. They suggested that the continue c^*/a^* ratio after ordering is complete due to the loss of the ZnO. Loss of ZnO is greater on the surface compare with the bulk because slow diffusion rate of Zn through the dense ceramic.

However, BZT was a particular interest for microwave applications because it can be fabricated with exceptionally high Q values at microwave frequencies. The microwave dielectric properties of BZT is affected by its structure. The ordering of B site cations has been influence the Q values of BZT ceramics (Varma et al., 2005). For pure BZT, high temperature for sintering was needed to achieve high Q values but sintering at temperatures above 1500°C leads to volatilization of ZnO and also increase the cost of manufacturing. The escape of ZnO led to poor densification and decreases the dielectric properties of BZT (Sebastian et al., 2008). To overcome these problems, other elements were added in the pure BZT. The adding of new elements also increases the dielectric properties. It has been reported by Kim et al. (2004) that addition of small amount of 1 mol% TiO₂ and 0.75 mol% Al₂O₃ can improve the Q and ϵ_r values of the materials. Another study, Jeong et al. (2005), found that extra addition of 0.3 mol% Ta₂O₅ can also increase dielectric properties. For example, a small amount of Ta₂O₅ can improved the Q values and the 1:2 order structure still maintain without changing to 1:1 ordering. Lee et al. (1998) found that lanthanum (La) substitution at the A site in BZT decreased the 1:2 ordering and at higher concentrations transformed to 1:1 ordered phase. For all dopants, grain growth occurred. The increase in Q values for small amount of doping is attributed to increase in density and grain growth (Jeong et al., 2005). However, the large addition amount of dopants elements (>2mol %) can decrease the density and Q values of BZT (Daevies et al., 2008).

Varma et al. (2005) made an investigation on the effect of dopant addition in the BZT. They added several dopants of varying valencies, ionic size and concentrations and studied the variations in densification, and microwave dielectric properties. It was

found that the Q values increased when the ionic radii of the dopant is close to that of B-site ions (Zn or Ta). The Q values increased when the ionic radii of the dopant is close to that of Zn (0.74 Å) or to that of Ta (0.64 Å). An amount of 0.5 mol% of Mg, Ni, Cr, In, Ga, Sn, Zr, Ce, Mn, and Sb improved the Q. values When the amount of dopant was increased to 1 mol%, the Q values were found to increase only for Cr, Ga, Zr, Ce, and Sn. The highest Q values were found for doping with Zr, Cr and Ce. In the doped samples the Q values are very much improved although the order parameter is decreased. Since these dopants having ionic radii close to that of the B-site ions improve Q values, it implies that these dopants are substituting for Zn or Ta in BZT.

There are many methods that producing the electroceramic powder like BZT. Generally, powder mixing method selection are depends on manufacturing cost, technical needed and the ability of the choosing method to achieve the needed properties. McLaren et al. (1999) was prepared the BZT by hydrothermal methods. Varma et al. (2006) prepared BZT nanopowder by the decomposition of a citrate precursor gel. However, the sinterability of BZT ceramics that made from nanopowder was very poor and on the sintering at high temperatures cause depletion of ZnO and form second phase of BZT, BaTa₂O₆. Varma et al. (2006) succeed in sintering BZT ceramics from nanopowder by using solid state method. Therefore, the solid state method is the cheapest method to produce this dielectric material. It is because this method is the cheapest manufacturing cost and simple procedure compare with sol gel and hydrothermal synthesis. Even though sol gel and hydrothermal synthesis can solve the high processing temperature problem but the quantity that produce is in small volume and the cost for these methods also expensive. Kong et al. (2007) stated that the

weakness of using sol gel is due to expensive alkoxide metal as a starting material and very sensitive with environment such as heat, light and moisture. Moisture sensitivity means the experiment must be conducted in vacuum room. So, the final product in a big amount is difficult to produce (Warikh et al., 2008).

1.2 Problem Statement

Complex perovskites $Ba(B'_{1/3}B''_{2/3})O_3$ compounds are very promising materials for electroceramic applications due to their attractive properties. The important characteristics required for DR are high ϵ_r and low $\tan \delta$ (Sebastian et al., 2008). BZT compound with excellent dielectric properties has been selected because of the potential applications in satellite broadcasting at frequencies higher than 10 GHz. Zirconia tin titanate, $(Zr_{1-x}Sn_x)TiO_4$, BZN and $Ba(Mg_{1/3}Ta_{2/3})O_3$ (BMT), having high ϵ_r are also widely used as a DR but these materials are not suitable in high frequency applications due to high $\tan \delta$ at high frequency range (Sebastian et al., 2008). Therefore, BZT is the best materials due to the stability of its properties in high frequency range.

The formation of BZT materials into dense ceramic resonators with excellent dielectric properties required very careful and demanding processing procedures because BZT is difficult to optimize on a commercial scale. This is a significant problem related to the BZT production cost. The atomic scale structure of BZT depends on the processing conditions since they control the extent to which the octahedral B-sites of the parent simple perovskite are occupied in an order manner by the Zn and Ta cations (Bieringer et al., 2003). The most common method that always uses to produce complex perovskites is solid state method. Even though this method is the easiest and the

cheapest method compare to the sol-gel, hydrothermal and etc., this method is still dealing with the high sintering temperature and long soaking time to produce very excellent dielectric properties. BZT has to be sintered at high temperature (1550°C) and long soaking time (120 hours). However, this procedure will also leads to volatilization of ZnO and increase the manufacturing cost. The escape of ZnO led to poor densification and decreases the dielectric properties of BZT (Cava et al., 2001). To overcome these problems, many researchers tried to dope BZT with many elements, respectively. It has been reported by Kim et al. (2004) that addition of small amount of 1 mol% TiO₂ and 0.75 mol% Al₂O₃ can improve the Q and ϵ_r values of BZT. Another study found that extra addition of 0.3 mol% Ta₂O₅ can also increase dielectric properties (Jeong et al., 2005). For example, a small amount of Ta₂O₅ can improved the Q values and the 1:2 order structure still maintain without changing to 1:1 ordering. Lee et al. (1997, 1998) found that lanthanum (La) substitution at the A site in BZT decreased the 1:2 ordering and at higher concentrations transformed to 1:1 ordered phase. Most of the researchers are successfully produce good dielectric properties compare to the pure BZT but the problem that involved with high sintering temperature is still cannot be solved. If they can sintered in short soaking time (6 to 10 hours) they still required high sintering temperature (>1550°C) in order to produce excellent dielectric properties (Sebastian et al., 2008).

The reason of using CaO, CuO and V₂O₅ is that these dopant have never been reported in previous literature. However, these dopants have been used in many materials such as BaTiO₃ (Moura et al., 2007), bismuth sodium titanate (Bi_{0.5}Na_{0.5}TiO₃, BNT) and barium zirconate titanate (Ba(Zr_{0.07}Ti_{0.93})O₃, BZT), Bi₂O₃-ZnO-Ta₂O₅

(Shen et al., 2004), bismuth based pyrochlores (Iqbal et al., 2010) and produce excellent dielectric properties at low sintering temperature. CaO is introduced as a doping compound because the Ca substitution form a new structured and avoid deteriorated microwave dielectric properties in high frequency range. CaO also exhibits high radiation resistance and also produce high ϵ_r . While, adding CuO can avoid Zn evaporation problem which lower the dielectric properties. The selection of V₂O₅ as a doping compound is to improve BZT dielectric since V₂O₅ has a relatively low melting point and can produce excellent dielectric properties. Therefore, with appropriate compositional design and selection of sintering temperature and duration, there is a possibility to decrease the sintering temperature and soaking time without Zn vaporization and produced BZT with excellent dielectric properties.

1.3 Research Objective

This study is focusing on dielectric properties of doped BZT and characterization of the BZT doped by various elements using solid state method. Therefore, the main objectives are:

- i. To investigate the lowest calcination temperature for producing single phase of BZT using solid state method.
- ii. To study the effect of reducing sintering temperature of BZT by doping with CaO, CuO and V₂O₅ respectively
- iii. To study the dielectric properties of BZT doped with CaO, CuO and V₂O₅ , respectively.

1.4 Scope of Work

Basically, this study can be divided into 3 phases which are:

- i. Finding the lowest calcination temperature to produce single phase of BZT using solid state method.
- ii. Reducing the sintering temperature of BZT by doped-BZT with CaO, CuO and V₂O₅ respectively.
- iii. Studying the dielectric properties of doped-BZT.

In the first phase, the solid state method used by other researchers such as Kawashima et al. (1983), Kim et al. (2001), Roulland et al. (2003) and Zaou et al. (2005) to produce BZT was employed. However, survey of the literature has not revealed any researcher using exactly the same chemicals in synthesizing a BZT doped CuO, CaO and V₂O₅ powder. Hence, these doped elements are seemed to be a newly elements developed during this thesis work. For the calcination process, the pure BZT powders obtained from the solid state method were calcined in a furnace at various temperatures ranging from 750 to 1250°C. The powders, calcined at different temperatures were then examined for their phase(s) content.

For the second phase, the BZT produced from the first phase was pressed and sintered at 1250°C, 1300°C and 1350°C in 4 hours soaking time, respectively. This is to determine the reference sintering temperature for pure BZT. Meanwhile, the BZT that produced from the first phase doped with 0.1 to 2.5 mol % of CuO, CaO and V₂O₅. The mixture were then calcined at 1150°C in 1 hour soaking time before being pressed into

pellets and sintered in three different sintering temperatures at 1200°C, 1250°C and 1300°C in 4 hours soaking time, respectively.

While, for the third phase, the final product of the doped-BZT were analyzed using network analyzer to investigate the doped-BZT microwave dielectric properties.

Characterization work was carried out after finding the optimum sintering temperature. Different properties of the sintered doped BZT such as grain size and microstructure, density, phase formation, resistivity, shrinkage and dielectric properties were examined with various analytical equipments such as Field Emission Scanning Electron Microscopy (FESEM), network analyzer and etc.

CHAPTER 2

LITERATURE REVIEW

2.1 Microwave Communications

Electromagnetic waves travel in a straight line at approximately the speed of light and are made up of magnetic and electric fields that are the right angles to each other and at right angles to the direction of propagation (Tomasi et al., 2004). Modern microwave and radio frequency (RF) engineering were widely used due to the explosion in demand for voice, data and video communication capacity (Golio et al., 2001). Microwave technology almost controlling the communication industry because increase in demand for communications systems such as mobile telephony, broadcast video and GPS to environmental monitoring via satellites (Golio et al., 2001). Most of the microwave based device systems are located from the range 300 MHz to 300 GHz as shown in Figure 2.1 (Golio et al., 2001). The microwave region can be divided into three sections, ultra high frequency (UHF) region from 300 MHz to 3 GHz, super high frequency (SHF) region from 3 GHz to 30 GHz and extremely high frequency (EHF) region from 30 GHz to 300 GHz (The Spectrum Plan, 2006). Compare with the radio waves, microwave can carried much more information because they have higher frequency and shorter wavelength (λ). Higher frequency can produce large BW that can achieve higher data transmission rates while the short λ allows the energy to be concentrated into a small area.

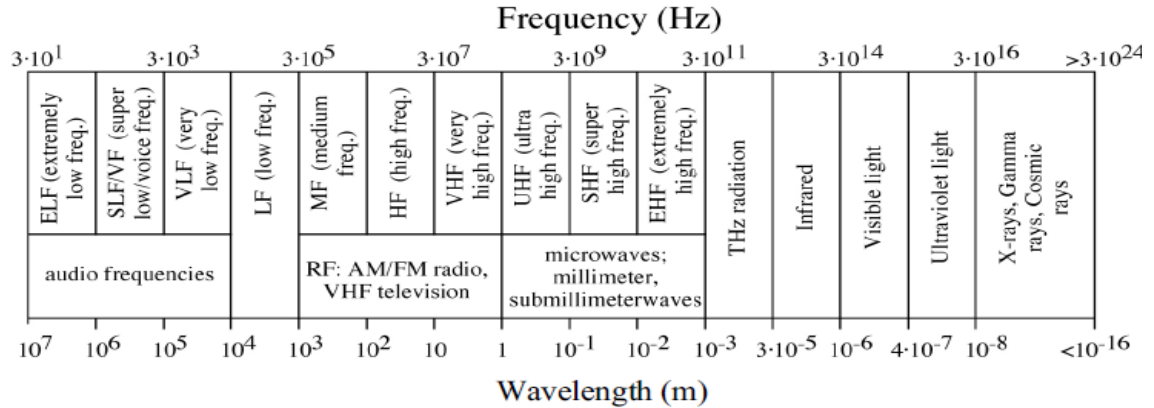


Figure 2.1: Microwave spectrum and applications (Golio et al., 2001).

2.1.1 Dielectric Resonators (DR)

A DR is an electromagnetic component that exhibits resonance with useful properties for narrow range of frequencies (Sebastian et al., 2008). DR is always used as a filters and oscillators. Richinger et al. (1939) showed that microwaves resonators in the form of unmetallized dielectric objects can function similarly to bulk metallic cavities and in late 1960s, the DR started to be used due to the development of low $\tan \delta$ ceramics materials. A DR tends to resonate at the frequency of the carrier signal to allow the signal to be efficiently separated from other signals in the microwave band; this frequency is called the f . The f depends on the dielectric material and the size of the resonator.

Around 1960s, many researchers investigated the behavior of dielectrics at microwave frequencies including Okaya et al. (1962), Barash et al. (1962), Coleman et al. (1960), Hakki et al. (1960) and Cohn et al. (1968). Many problems occurred at that time due to the limited number of the suitable materials. The first DR was in the form of TiO_2 single crystal (Khisk et al., 2007). Rutile (TiO_2) has high ϵ_r and low $\tan \delta$ but its

large f of the temperature coefficient made it impractical for many applications. By the 1970s, the commercialization of DR for real applications had begun introduced to the worldwide.

2.1.2 Dielectric Resonator Antenna (DRA)

Several DR can fabricate to form DRA. DRA can produce high degree of flexibility and versatility over a wide frequency range that suit many requirements. DRA offer many advantages. First, the DRA size is proportional to the $\lambda_0 / \sqrt{\epsilon_r}$ where ϵ_r the dielectric constant of the DRA and λ_0 is the wavelength of the f . The different values of ϵ_r (range from 4 to 100) can be used. Therefore, it gives the flexibility to control the size and BW (Khisk et al., 2007). Second, DRA has much wider impedance BW compare with microstrip antenna. Compared with microstrip antenna, DRA can radiate through the whole antenna surface except the grounded part while microstrip antenna can radiates only through narrow radiation slot (Khisk et al., 2007). The DRA operating BW can be varies by choosing suitably ϵ_r of resonator material and its dimensions. Third, DRA consists high dielectric strength and high power handling capacity. This antenna can operate in wide temperature range due to the temperature stable ceramics.

There are three major of important properties that need to be considered to choose the materials for DRA. The ϵ_r controls the resonator dimensions and should be as high as possible. A low $\tan \delta$ is very important for high performance devices because the lower $\tan \delta$, the higher the efficiency and lower the noise (Pern et al., 1999). To increase the efficiency of DR in telecommunication applications, low return loss and high BW are required.

2.1.2.1 Effect of DRA Height and Shape

The mode of operation and performance of a DRA can be varied by selecting a DR with desired structure. The systematic research already been conducted in 1983 and 1984 towards the different shape of DRA such as cylindrical, hemisphere, and rectangular shape (Long et al., 1983). Each of these shape were characterized with the value of ϵ_r , radius (a), height (h), and thickness (d). Mridula et al. (2004) state that the different between h and width (w) for rectangular DRA give an effect to the f and return loss.

Figure 2.2 shows those two units of DRA that have different h which is DR₁ and DR₂. The f for DR₁ exist at 1.795 GHz with 6.12% BW and suitable to operate at GSM 1800 (1710-1880 MHz) frequency. While, the f for DR₂ occurred at 2.445 GHz and it is suitable to operate in wireless local area network (WLAN) frequency (2.4-2.484 GHz). In Figure 2.3, two units of DRA that have different BW which is DR₃ and DR₄. For DR₃, it is suitable for GPS band (1.565-1.585 GHz) and for DR₄ for PCS 1900 band (1.85-1.99 GHz). These results show that different dimension of DR can produce different f for different applications.

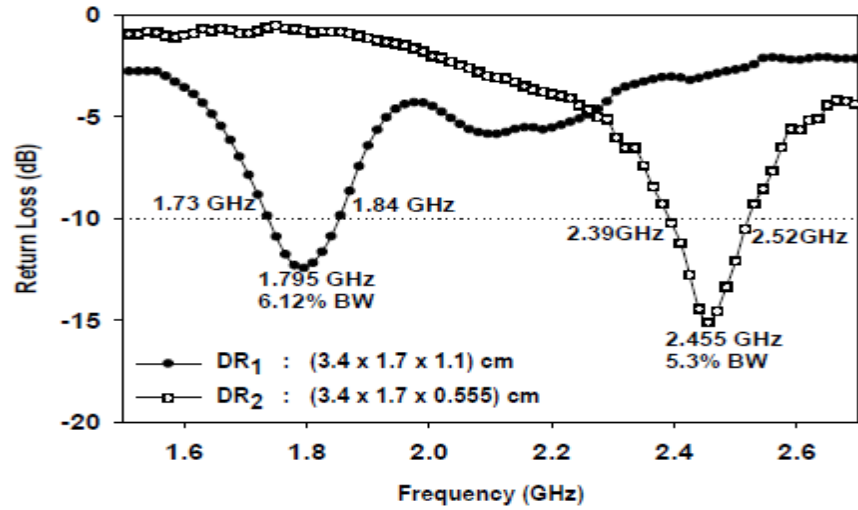


Figure 2.2: Return loss for antenna with two samples different h (Mrindula et al., 2004)

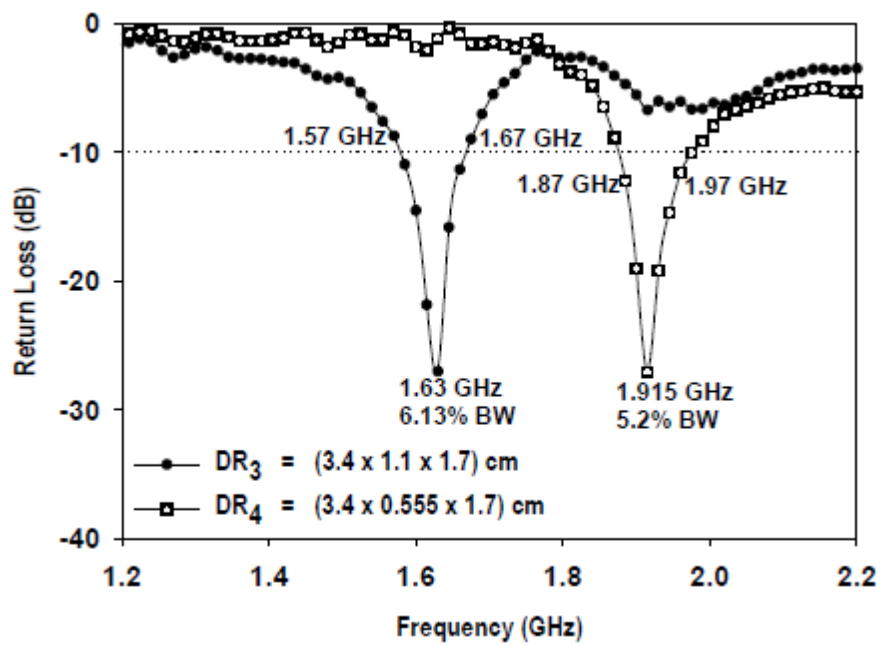


Figure 2.3: Return loss for antenna with two samples different BW (Mrindula et al., 2004)

2.1.2.2 The Hemispherical DRA

The geometry of the hemispherical DRA is shown in Figure 2.4. The hemispherical DRA is of limited practical value. It is because due to the difficulty involved in fabrication and lack of any degree freedom in choosing the design parameters. For the materials that have certain ϵ_r , the radius of sphere will determine both the f and the radiation that will produce. Therefore, the designer cannot control the size of the antenna and its BW. The designer has difficulty to control the size of antenna or BW due to the limited characterization.

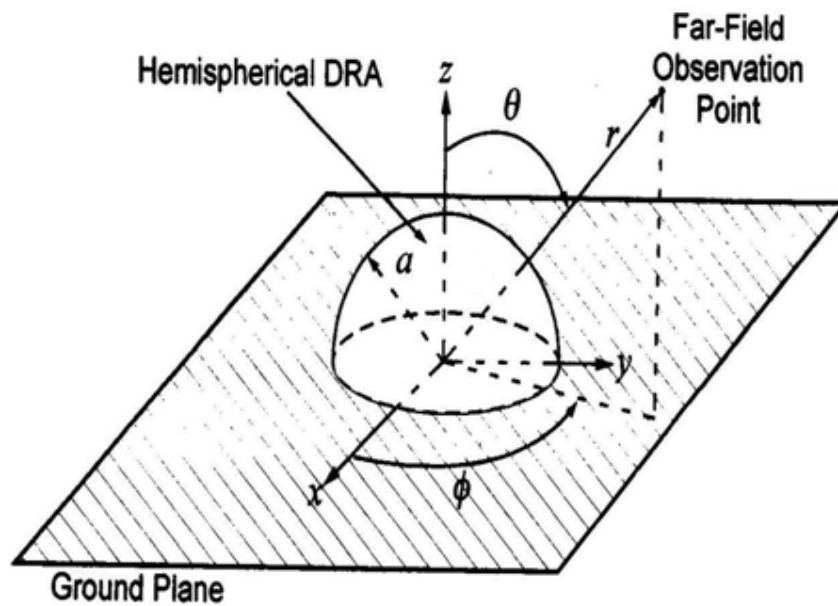


Figure 2.4: Hemispherical DRA (Petosa et al., 2007)

2.1.2.3 The Rectangular DRA

The DRA with a rectangular cross section is characterized by h , w , d , and ϵ_r as shown in Figure 2.5. The rectangular shape offers a second degree of freedom which is h/w and d/w making it most versatile of the basic shape. There is greater amount of flexibility in designing the rectangular DRA to achieve desired profile and BW characteristics for a given f and ϵ_r since the ratio of (d/w) and (h/w) can be chosen independently. The choice of aspect ratio will also have an impact in the radiation. Thus, it allowed the designer to make many choices to design the DRA for certain application.

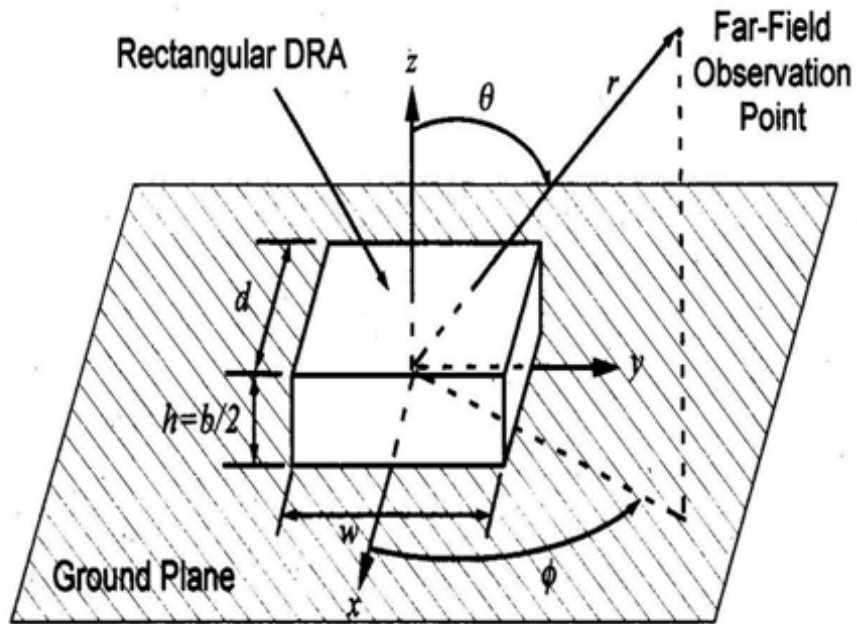


Figure 2.5: Rectangular DRA (Petosa et al., 2007)

2.1.2.4 The Cylindrical DRA

The cylindrical DRA offers greater design flexibility, where the ratio of a/h controls the f and dielectric properties. So, for a given ϵ_r and f , different $\tan \delta$ can be obtained by varying the DRA dimensions. Fabrication is also simpler than the hemispherical DRA. The cylindrical DRA is characterized by h , a , and ϵ_r as shown in Figure 2.6. The cylindrical shape offers one degree of freedom more than hemispherical shape which is the aspect ratio a/h . Thus, the cylindrical DRA can be made to resonate at the same frequency as a wide and thin cylindrical DRA. However, the $\tan \delta$ for both resonators is different. DRA that use for electronic circuit usually been produce in cylindrical shape or pellet that have high $\epsilon_r (>35)$ (Long et al., 1983).

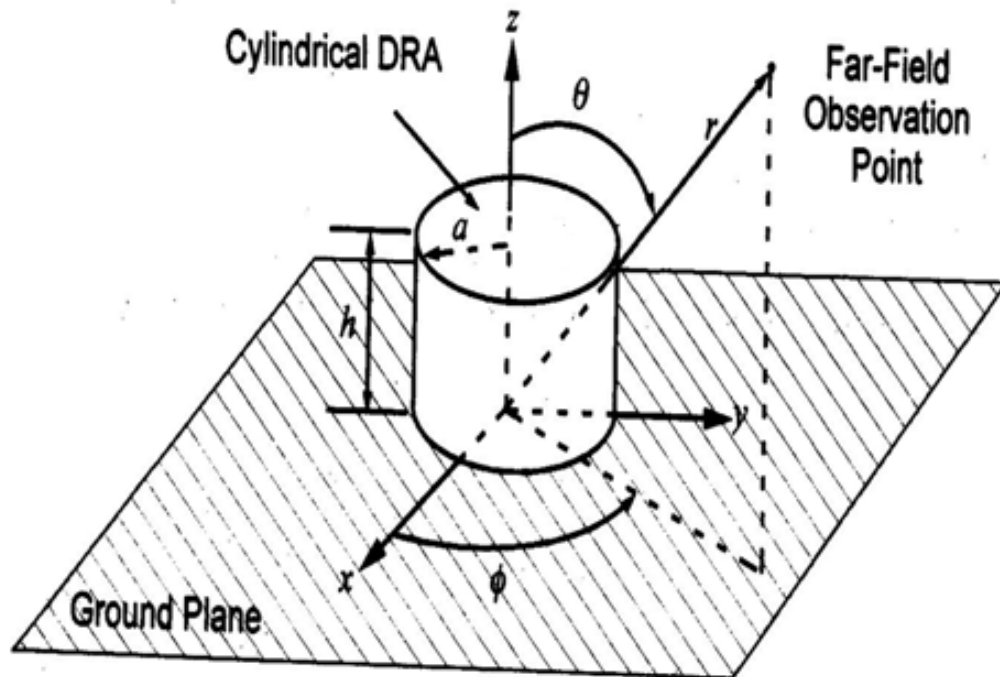


Figure 2.6: Cylindrical DRA (Petosa et al., 2007)

2.1.3 Dielectric Microwave Properties

2.1.3.1 Dielectric Resonance Frequency (f)

The f is the frequency which capacitance and inductance are cancelling to each others. The f of a DR in the $HE_{11\delta}$ mode can be estimated by Equation 2.1 formulated by Long et al. (1988).

$$f = \frac{6.324c}{2\pi a\sqrt{\epsilon_r} + 2} \left[0.27 + 0.36 \left(\frac{a}{2d} \right) + 0.02 \left(\frac{a}{2d} \right)^2 \right] \quad (2.1)$$

where;

f = Resonance frequency

ϵ_r = Dielectric constant

a = Radius of resonator (m)

d = Thickness of resonator (m)

The f can be changed by altering the dimensions of DR. f increase when the size of DR decreases and ϵ_r values are low.

2.1.3.2 Dielectric Constant (ϵ_r)

The ϵ_r is the degree of polarizability or energy storing capacity when the potential is applied across it. High ϵ_r values were needed for circuit miniaturization. This is because the λ inside the DR is inversely proportional to the square root of its ϵ_r as given by the Equation 2.2.

$$\lambda_d = \lambda_o / \sqrt{\epsilon_r} \quad (2.2)$$

Where;

λ_d = Wavelength in dielectric

λ_o = Wavelength in air

ϵ_r = Dielectric constant

High ϵ_r values can reduce the size of the antenna. A relatively small antenna can efficiently radiate high frequency electromagnetic wave. When $\sqrt{\epsilon_r}$ increase, the λ_d will decrease and when the microwave frequency enter the dielectric material, the length of λ will decrease and produce short λ that performed better frequency as shown in Figure 2.7. Materials with low ϵ_r values are used for electrical insulator applications. Materials with high ϵ_r values are used as a DR or capacitors for charge storage and other function.

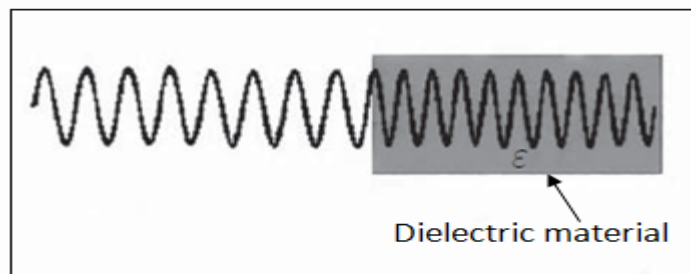


Figure 2.7: The λ is reduced by factor of $\sqrt{\epsilon_r}$ when the waves enter the dielectric material (Sebastian et al., 2008)

Polarization happens when an electric field is applied to a dielectric material, there are no long range of transport of charge of material but the charge of material are displaced in response to the applied field. The orientation of the charge reduce the effective of electric field between the plates because the charged tied up charges on the plate of the condenser but it increase the ability of the plates to store charge. Relaxation time was needed to achieve the equilibrium orientation and relaxation frequency as a reciprocal for relaxation time.

Figure 2.8 shows various types of polarization. At the highest frequencies (10^{13} to 10^{15} Hz), the electron is the polarizing species in a material. Electronic polarization occurs when an applied electric field causes the shift of the electron cloud. Ionic polarization occurs at frequencies below 10^{13} Hz and this is due to the displacement of positive and negative ions with respect to each other (Nair et al., 2002). Below 10^{10} Hz, orientation polarization occur because molecules that contain permanent dipole rotating between the two equivalent equilibrium positions and space charge polarization that produced at frequencies below 10^5 Hz form due to the mobile charge carriers that are impeded by physical barrier (Nair et al., 2002).

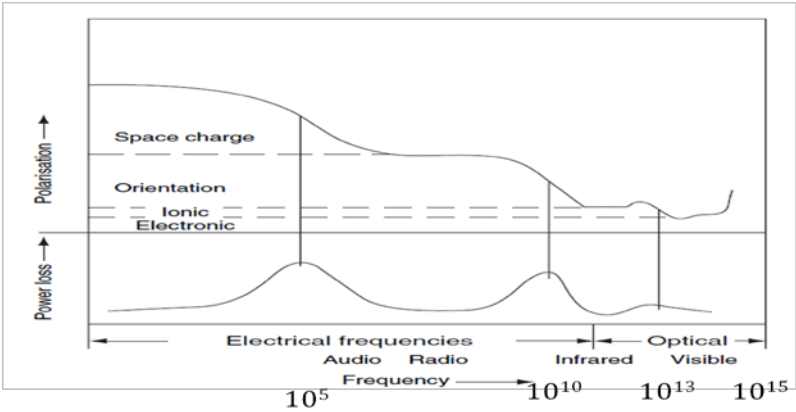


Figure 2.8: Frequency dependence of polarization process and peak power losses (Sebastian et al., 2008)

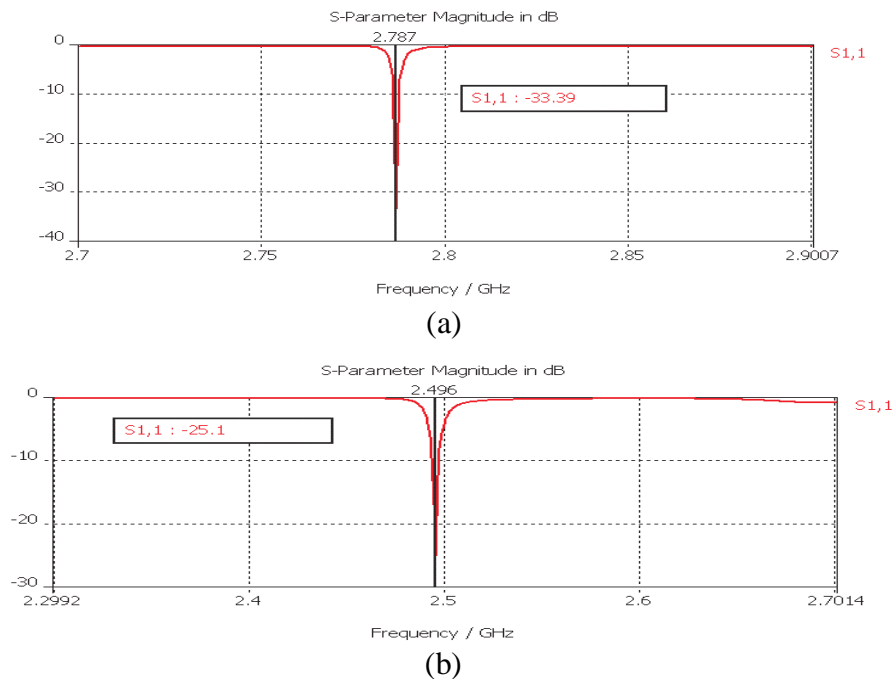
2.1.3.3 Dielectric Loss ($\tan \delta$)

Due to the different physical processes such as dielectric resonance, electrical conduction and dielectric relaxation, the $\tan \delta$ of a material denotes quantitatively dissipation of the electrical energy (Bartfoot et al., 1967). The total $\tan \delta$ is the sum of the intrinsic and extrinsic losses. The intrinsic losses are dependant on the composition of the material while the extrinsic losses are the additional losses due to the imperfections in crystal structure. The losses are determined by the phonon interactions in ideal crystals, impurities, vacancies, porosity, grain boundaries and dopants in real materials.

The intrinsic losses happen due to the anharmonic lattice forces that control the interaction of phonon system. This is because the microwave frequency is lower than phonon frequency so the microwaves cannot directly interact with the individual phonons. From theory, lowest $\tan \delta$ can be achieved from a single crystal since defects and impurities can increase the phonon scattering. Extrinsic losses can be divided into two groups; 1) losses in real homogeneous single crystals causes by dopant, impurity and vacancies and 2) losses in inhomogeneous ceramics due to extended grain boundaries, vacancies and second phase. The losses from point 1 can be seen as energy transfer from the excited microwave to transverse optical phonons. Through scattering and interaction with other phonon, thermal phonons can be generating from these optical phonons.

2.1.3.4 Minimum Return Loss

Minimum return loss is a portion of a signal that cannot be absorbed by the end of line termination, or cannot cross an impedance change at some point in the transmission system. Minimum return loss value must less than -10 dB. The minimum return loss is influence by the thickness of the DRA. It proves by Ain et al. (2007) that use different thickness of resonator were produced different operation of f . Based on Figure 2.9, the minimum return loss decreased when the thickness of DR decrease. Therefore, the minimum return loss values indicated that by reduce the thickness of DR can minimize the return loss during the operation. This suggests that with low value of minimum return loss, this DR has very good efficiency in a telecommunication system. This result also proven that the f can be achieved by modified the resonator from many aspect such as thickness, sintering time and dopants.



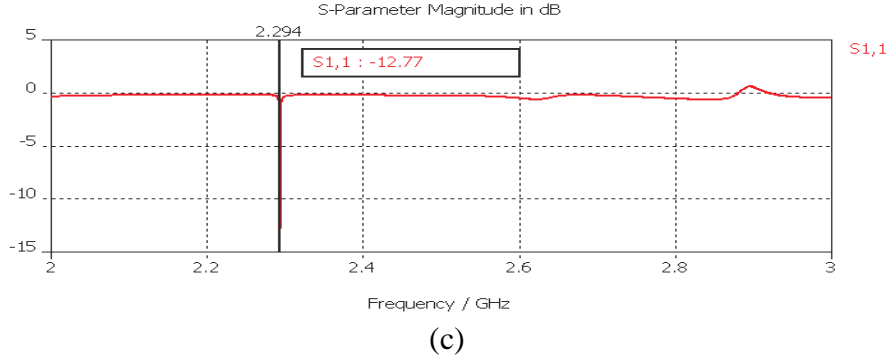


Figure 2.9: Thickness effect for the DR towards return loss. (a) 2 mm, (b) 2.5 mm (c) 3 mm (Ain et al., 2007)

2.1.3.5 Bandwidth (BW)

BW is a total distance or range between the highest and lowest frequency of acceptable operation and multiplied by 100 and represented by % BW as in Equation 2.3.

$$\% BW = \frac{f_2 - f_1}{f_c} \times 100 \quad (2.3)$$

Where;

f_1 = lower frequency limit where the magnitude of the spectrum is 10 dB weaker than the strongest frequency component in the whole occupied spectrum.

f_2 = higher frequency limit where the magnitude of the spectrum is 10 dB weaker than the strongest frequency component in the whole occupied spectrum.

f_c = center frequency defined as the averaged between the higher frequency limit and the lower frequency limit divided by 2.

For both higher and lower frequency limits are taken at -10 dB levels. It is because the BW can be accepted when the specific range of the frequencies over which antenna is capable of transmitting and receiving signals above -19 dB relative to the strongest frequency component in the entire spectrum

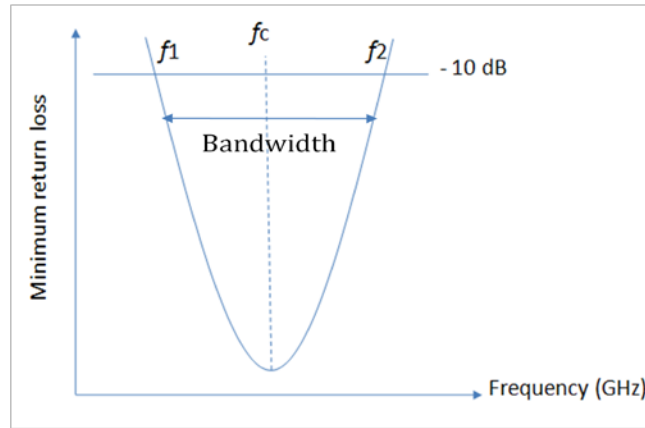


Figure 2.10: Measurement of BW based from the f

The resonator BW is depends on the f , ϵ_r , $\tan \delta$ and the thickness (d) of the pellets. But in this research the scope are more in f and the ϵ_r . The BW and ϵ_r are interrelated; therefore there is always a trade off between them in arriving at optimum dielectric properties for telecommunication applications.

2.2 Perovskite Structure

The structural chemistry of ABO_3 perovskites can be described in terms of close packing of AO_3 layers, where at the B-sites cations occupy 100% of resultant BO_6 oxygen octahedra. The BO_6 octahedra is connected exclusively through corner sharing when the AO_3 layers are arranged in cubic close packing and then, the structure form in a cubic perovskite. In an ideal cubic perovskite, the A and B cations have an equilibrium bond distances to oxygen without any distortion of the unit cell. So, it was classified in the space group $Pm\bar{3}m$ and the tolerance factor, $t = 1$ (Long et al., 1983).

As shown in Figure 2.11, the B atoms are at the center of 6 oxygen that are arranged at the corner of a regular octahedron. The octahedra are linked at their corner into a three dimensional simple cubic network, enclosing large holes that are occupied